Phase separation and dilution in implanted Mn_xGe_{1-x} alloys

L. Ottaviano,[a] M. Passacantando, S. Picozzi, and A. Continenza
CNISM-C.N.R. and Dipartimento di Fisica, Università degli Studi dell'Aquila, I-67010 Coppito (L'Aquila), Italy

R. Gunnella
Dipartimento di Fisica, Università di Camerino, Via Madonna delle Carceri, 62032 Camerino MC, Italy

A. Verna
Dipartimento di Fisica, Università di Padova, Via F. Marzolo 8 I-35131 Padova, Italy

G. Bihlmayer
Institut für Festkörperforschung, Forschungszentrum Jülich, D-52425 Jülich, Germany

G. Impellizzeri and F. Priolo
MATIS-CNR-INFN and Dipartimento di Fisica e Astronomia, Università di Catania, I-95123 Catania, Italy

(Received 28 July 2005; accepted 13 December 2005; published online 7 February 2006)

The structural and electronic properties of Mn_xGe_{1-x} alloys ($x \leqslant 0.15$) fabricated by ion implantation are investigated by means of x-ray diffraction and synchrotron radiation photoemission spectroscopy. The diffraction patterns point to the presence of ferromagnetic Mn_5Ge_3 nanoparticles; however, valence band spectra, interpreted by means of accurate *ab initio* calculations including Hubbard-like correlations, show clear fingerprints of an effective substitutional Mn dilution in the Ge semiconducting host. © *2006 American Institute of Physics*. [DOI: 10.1063/1.2171485]

The achievement of ferromagnetism (FM) in Ge by inclusion of magnetic dopants (Mn, Cr, Fe) has attracted considerable attention due to its full compatibility with the mainstream silicon technology.[1] However, the magnetic response of most of the Mn_xGe_{1-x} alloys realized so far is due to Mn-rich separated phases,[2,3] and only few are indicative of an efficient dilution.[1,4] An homogeneous distribution of magnetic impurities in the semiconducting (SC) matrix is a fundamental requirement to obtain, at the same time, SC functionalities and magnetic order.[5] On the other hand, phase separation (i.e., formation of metal-rich precipitates showing FM at room temperature), is also extremely interesting on its own both from a fundamental as well as from a technological standpoint.[6] The investigation of the structural and electronic properties of the alloy—as a function of the Mn concentration x and of the interplay between the two above-mentioned regimes—is therefore of primary interest for a full understanding of the magnetic properties.[6]

Ion implantation at a fixed beam energy produces implanted films with varying concentration profiles. This apparent intrinsic limitation becomes an advantage as concentration dependent investigations can be performed on a single sample. Here we report on a systematic experimental and theoretical study as a function of Mn x concentration of the structural and electronic properties of ion implanted Mn_xGe_{1-x} alloys ($0.01 < x < 0.15$).

Chemically cleaned intrinsic Ge(100) single crystal wafers were implanted with 100 keV Mn^+ ions at two different doses of 4×10^{16} and 2×10^{16} at./cm^2 at a substrate temperature of 300 °C to avoid amorphization (as in Ref. 7). The samples have been studied with: x-ray diffraction (XRD) (Siemens D5000 diffractometer with Cu $K\alpha$ radiation) operating in the Bragg–Brentano mode, standard x-ray photoemission (PE) spectroscopy for depth profiling (XPS, ESCA PHI 1257), and synchrotron radiation PE for valence band (VB) investigation (VUV Beamline ELETTRA, Trieste). Accurate first-principles calculations have been performed within the generalized gradient approximation to the density functional theory, using the full-potential linearized augmented plane wave method in the FLEUR implementation.[8]

Figure 1(a) shows the XPS depth profile characterization of the Mn_xGe_{1-x} samples, after absolute calibration of the Mn/Ge relative cross section on a Mn_5Ge_3 550-Å-thick film molecular beam epitaxy (MBE) grown on Ge(111).[9] The Mn peak concentrations are 0.15 ± 0.01 and 0.09 ± 0.01 for the two different doses of 4×10^{16} and 2×10^{16} at./cm^2, respectively. These values are significantly larger than those typical of diluted magnetic semiconductors. The Mn distribution profiles are asymmetric with positive skewness and with the same parameters for projected range (50 ± 5 nm), and end of range 130 ± 5 nm. Figure 1(b) shows the XRD spectra of the implanted Mn_xGe_{1-x} samples. Beside the (200) at 31.67° and (400) at 66.018° diffraction peaks of the Ge matrix, there is a diffraction peak at 35.45° (also non negligible for the 2×10^{16} at./cm^2 case). This is the (002) peak relative to the Mn_5Ge_3 phase,[9,10] easily distinguishable from the (002) $Mn_{11}Ge_8$ phase at 0.2° lower diffraction angle. Considering the relative Mn/Ge concentrations of Fig. 1 evidently the Mn_5Ge_3 diffraction peak is due to phase separation into Mn-rich clusters embedded in the Ge matrix. By means of the Scherrer formula, a detailed analysis after acquisition with high signal-to-noise ratio of the spectral region around this peak allows determination of the average cluster sizes, that are 12 ± 1 and 8 ± 1 nm for the two doses of 4×10^{16} and 2×10^{16} at./cm^2, respectively. Worth noting is that the estimated volume ratio of the clusters in the two implanted alloys is $(8/12)^3 \simeq 0.3$. This is significantly lower than the 1:2 ratio expected from the doubling of the Mn dose in the two alloys. This indicates that, with halving the Mn dose in the

[a]Author to whom correspondence should be addressed; electronic mail: luca.ottaviano@aquila.infn.it

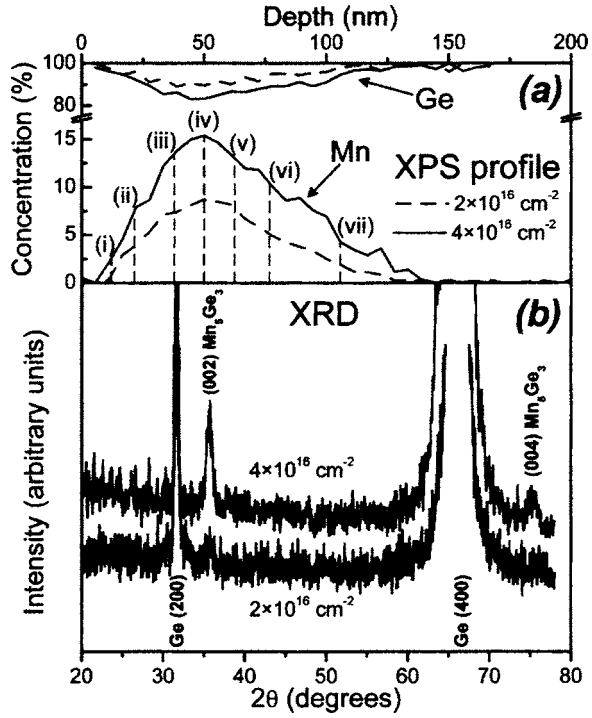

FIG. 1. (a) XPS depth profiles showing the in-depth Mn concentration for the 4×10^{16} (solid curve) and 2×10^{16} (dashed curve) Mn ion doses in Ge(001) implanted samples. Upper curves: corresponding Ge concentrations. The vertical dashed lines on the 4×10^{16} alloy curve indicate the depths of subsequent sputtering in correspondence of which the valence band spectra have been taken (see Fig. 2). (b): XRD patterns for the two ion implanted MnGe samples.

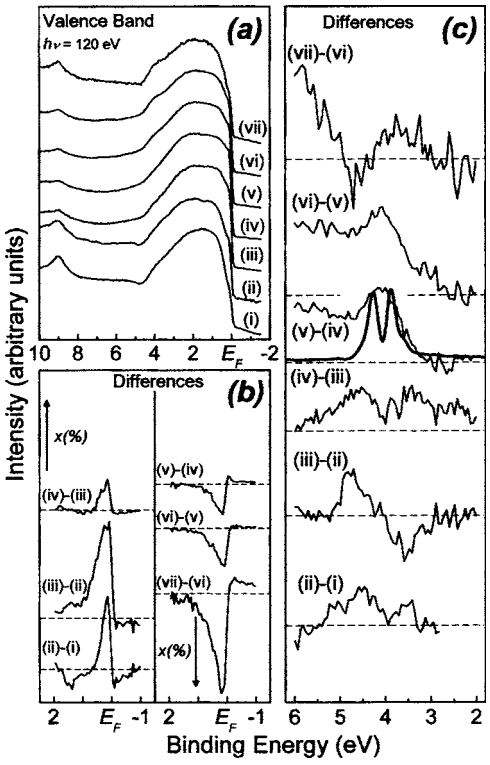

FIG. 2. (a) Valence band spectra taken on the 4×10^{16} Mn ion dose sample at various depths (Mn surface concentration, see Fig. 1) after seven subsequent sputtering cycles (spectra are normalized to unit at their common peak energy value at 2.0 eV). (b) and (c) Corresponding incremental difference spectra (horizontal dashed lines are the corresponding zero levels). The solid curve superimposed on the (v)-(iv) data in (c) is the Mn projected DOS for substitutional Mn in Ge [see Fig. 3(a)].

implanted region, there is a less effective migration of Mn into phase separated Mn-rich clusters with a significant fraction of Mn presumably diluted in the Ge matrix. This evidence of phase coexistence is clarified and strenghthened by our VB PE investigation. In this case we focused on the 4×10^{16} at./cm^2 dose that allowed to span the larger x range.

Figure 2(a) reports, from bottom to top, the VB spectra obtained after seven subsequent sputter (2.0 keV) annealing (200 °C) cycles (estimated etch rate 1.8 nm/min), each one stopped at the following estimated depths with respect to the pristine nonsputtered surface [see dashed lines in Fig. 1(a)] (i) 11 nm, (ii) 22 nm, (iii) 38 nm, (iv) 50 nm, (v) 63 nm, (vi) 77 nm, and (vii) 106 nm, corresponding to Mn concentration values of 0.025, 0.08, 0.13, 0.15, 0.12, 0.10, and 0.05 respectively. The experimental settings ($h\nu$=120 eV, normal emission mode, 7° analyzer angular acceptance) are chosen so that the angle integrated electronic structure of the sample is probed with few nanometers in depth sensitivity. Indeed, from Fig. 1(a) an estimate of the average rate of in depth variation of x is 1.5×10^{-3} nm^{-1}, then each VB spectrum after each sputter annealing cycle can be really assigned to a fixed Mn concentration x.[11] A spectral signature of Mn_5Ge_3 precipitates is readily noticeable in all the VB spectra of Fig. 2(a): a high spectral density at the Fermi level (E_F). Both theory[12] and PE experiments on epitaxial Mn_5Ge_3[13] show a high density of the Mn d derived states at E_F. Since the Ge matrix is common to all sampled regions, the spectral information due to the variation of the Mn content in the Mn–Ge implanted sample can be more easily disentangled by means of the difference spectra as shown in panels (b) and (c) of the same figure. Such spectra give an experimental estimate of the Mn projected density of states (PDOS) of the alloy. In Fig. 2(b) there is a clear increase (decrease) of the density of states at E_F upon increasing (decreasing) x. This is assigned to an increase (decrease) with depth of the volume concentration of Mn_5Ge_3 crystallites in the host Ge matrix. In Fig. 2(c) the same difference spectra are reported in the region between 2.0 and 6.0 eV below E_F. The first three (from bottom to top) difference curves, obtained increasing x, show a hump centered at 4.8 eV in good agreement with a similar feature of the Mn_5Ge_3 phase.[13] Remarkably, when considering difference spectra related to a decrease in the Mn concentration a positive hump appears at 4.0 eV below E_F. If Mn was incorporated exclusively in precipitates, this experimental evidence would not be explained. Rather, only negative features would be expected. Evidently, as x in the alloy decreases, there is an increase of the spectral weight related to features that are typical of a Mn–Ge diluted alloy. Indeed, the experimental Mn PDOS of curves (v)-(iv), (vi)-(v) in Fig. 2(c) are very similar to those obtained in PE investigations of MBE Mn doped III-V SC like $Ga_{1-x}Mn_xAs$[14] and $In_{1-x}Mn_xAs$,[15] where Mn dilution in substitutional sites is claimed. Thus, comparison of our spectra with the Mn PDOS from *ab initio* calculation for a diluted MnGe alloy is worthwhile and enlightening.

In Fig. 3 we report the Mn PDOS for the substitutional and interstitial case, with and without introduction of Hubbard-like correlations. By symmetry, e orbitals very weakly hybridize with host-like states, whereas t_2 states form bonding-antibonding ($b-ab$) pairs with Ge p states in each spin channel.[16] Within general gradient approximation

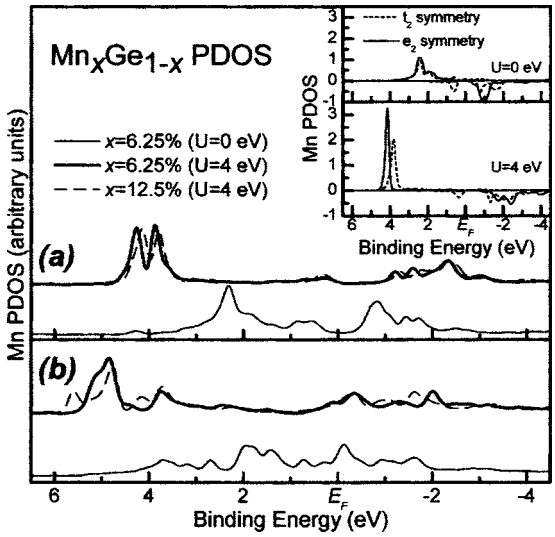

FIG. 3. PDOS of (a) substitutional and (b) interstitial Mn in Ge with and without U (upper and lower lines, respectively). Upon inclusion of U, the Mn PDOS for different concentrations (6.25% and 12.5%) is also reported. Inset: Orbital (t_2 and e) and spin resolved Mn PDOS.

(GGA) and without U, e^+ and t_b^+ states are fully occupied and lie in a similar energy range (~ -2 eV), as previously found;[17] the singly occupied t_{ab}^+ crosses E_F (giving rise to two holes, having both Mn d and Ge p character), whereas t_b^- lies just below E_F. Upon introduction of U, both e^+ and t_b^+ states are shifted towards higher binding energies and are remarkably localized in energy: the t_b^+ state is much less hybridized than in bare GGA and appears as an atomic-like peak, as the nonhybridized e state. As U is introduced, the Mn weight on the t_{ab}^+ state (and, as a consequence, on states close to E_F) is strongly reduced and the holes have a larger Ge p character. The Mn (total) magnetic moment changes from 3.2 μ_B (3.0 μ_B) to 3.8 μ_B (3.2 μ_B) without and with U, respectively. The Mn electronic configuration is therefore d^5+2 holes in both cases, but the hole acquires more Ge p-like character, losing Mn d weight. For Mn in Ge, there is an evident inadequacy of bare GGA (or local spin density approximation, as well) in reproducing the VB spectra and a GGA+U approach is needed,[18] with an estimate of the Hubbard parameter U from first principles[19] of about $U \sim 3-4$ eV.[20] Indeed, once the Hubbard parameter is set to $U=4$ eV, an excellent agreement is found between theory and experiment [see Figs. 3(a) and 2(c)] not only as for the energy position of the experimental data, but also for the peak width. This picture is kept upon variation of x: there are no basic differences in doubling (or halving, not shown) the transition-metal doping [see Fig. 3(a)]. Instead, similar GGA and GGA+U calculations for Mn_xGe_{1-x} alloys with Mn in the interstitial do not produce a good agreement even upon the necessary introduction of U. Thus our theoretical investigation gives strong indication that Mn is substitutionally diluted in the Ge matrix.

In summary, ion-implanted Mn_xGe_{1-x} alloys have been studied as a function of the Mn concentration, with XRD and VB PE. While x-ray diffraction reveals the presence of Mn_5Ge_3 ferromagnetic nanoparticles, the presence of a diluted Mn phase in coexistence with the cluster phase is clearly demonstrated with photoemission. In particular, comparison of VB data with *ab initio* GGA+U calculations show that a typical feature arising upon decreasing x (i.e., the peak at -4 eV in the PE spectra) can be considered as a fingerprint of effective dilution of substitutional Mn in the Ge matrix. We also demonstrated that ion implantation produces a significant effective Mn dilution into Ge even at extremely high doses of the magnetic impurities.

[1] Y. D. Park, A. T. Hanbicki, S. C. Erwin, C. S. Hellberg, J. M. Sullivan, J. E. Mattson, T. F. Ambrose, A. Wilson, G. Spanos, and B. T. Jonker, Science **295**, 651 (2002).
[2] S. Cho, S. Choi, S. C. Hong, Y. Kim, J. B. Ketterson, B.-J. Kim, Y. C. Kim, and J.-H Jung, Phys. Rev. B **66**, 033303 (2002).
[3] J.-S. Kang, G. Kim, S. C. Wi, S. S. Lee, S. Choi, S. Cho, S. W. Han, K. H. Kim, H. J. Song, H. J. Shin, A. Sekiyama, S. Kasai, S. Suga, and B. I. Min, Phys. Rev. Lett. **94**, 147202 (2005).
[4] A. P. Li, J. Shen, J. R. Thompson, and H. H. Weitering, Appl. Phys. Lett. **86**, 152507 (2005).
[5] Y. Ohno, D. K. Young, B. Beschoten, F. Matsukura, H. Ohno, and D. D. Awschalom, Nature (London) **402**, 790 (1999).
[6] R. Goswami, G. Kioseoglou, A. T. Hanbicki, O. M. J. van 't Erve, B. T. Jonker, and G. Spanos, Appl. Phys. Lett. **86**, 032509 (2005).
[7] D. P. Norton, S. J. Pearton, A. F. Hebard, N. Theodoropoulou, L. A. Boatner, and R. G. Wilson, Appl. Phys. Lett. **82**, 239 (2003).
[8] http:www.flapw.de
[9] R. Gunnella, L. Morresi, N. Pinto, R. Murri, L. Ottaviano, M. Passacantando, F. D'Orazio, and F. Lucari, Surf. Sci. **577**, 22 (2005).
[10] C. Zeng, S. C. Erwin, L. C. Feldman, A. P. Li, R. Jin, Y. Song, J. R. Thomson, and H. H. Weitering, Appl. Phys. Lett. **83**, 5002 (2003).
[11] Also routine AFM characterization indicates that the samples are atomically flat (0.1 nm mean surface roughness). After sputtering the surface roughness is of the order of 10 Å.
[12] S. Picozzi, A. Continenza, and A. J. Freeman, Phys. Rev. B **70**, 235205 (2004).
[13] C. Zeng, W. Zhu, S. C. Erwin, Z. Zhang, and H. H. Weitering, Phys. Rev. B **70**, 205340 (2004).
[14] H. Åsklund, L. Ilver, J. Kanski, J. Sadowski, and R. Mathieu, Phys. Rev. B **66**, 115319 (2002); J. Okabayashi *et al.*, *ibid.* **59**, R2486 (1999).
[15] J. Okabayashi, T. Mizokawa, D. D. Sarma, A. Fujimori, T. Slupinski, O. Oiwa, and H. Munekata, Phys. Rev. B **65**, 161203 (2002).
[16] A. Continenza, G. Profeta, and S. Picozzi, Phys. Rev. B (in press).
[17] Y.-J. Zhao, T. Shishidou, and A. J. Freeman, Phys. Rev. Lett. **90**, 047204 (2003).
[18] V. I. Anisimov, F. Aryasetiawan, and A. I. Lichtenstein, J. Phys.: Condens. Matter **9**, 767 (1997).
[19] M. Cococcioni and S. De Gironcoli, Phys. Rev. B **71**, 035105 (2005).
[20] S. Picozzi, F. Antoniella, A. Continenza, A. Moscaconte, A. Debernardi, and M. Peressi, Phys. Rev. B **70**, 165205 (2004).